Propagation of kink–antikink pair along microtubules as a control mechanism for polymerization and depolymerization processes*

L. Kavitha[a)b)†], A. Muniyappan[c)], S. Zdravković[d)], M. V. Satarić[e)], A. Marlewski[f)], S. Dhamayanthi[c)], and D. Gopi[g)h)]

[a)] *Department of Physics, School of Basic and Applied Sciences, Central University of Tamilnadu (CUTN), Thiruvarur* 610101, *India*
[b)] *The Abdus Salam International Center for Theoretical Physics, Trieste, Italy*
[c)] *Department of Physics, Periyar University, Salem* 636011, *India*
[d)] *Institut za nuklearne nauke Vinca, Laboratorija za atomsku fiziku* 040, *Univerzitet u Beogradu, Postanski fah* 522, 11001 *Beograd, Serbia*
[e)] *Fakultet tehnickih nauka, Univerzitet u Novom Sadu*, 21000 *Novi Sad, Serbia*
[f)] *Institute of Mathematics, Poznan University of Technology, Piotrowo 3A*, 60-965, *Poznan, Poland*
[g)] *Center for Nanoscience and Nanotechnology, Periyar University, Salem* 636011, *India*
[h)] *Department of Chemistry, Periyar University, Salem* 636011, *India*

(Received 4 October 2013; revised manuscript received 21 February 2014; published online 13 August 2014)

Among many types of proteinaceous filaments, microtubules (MTs) constitute the most rigid components of the cellular cytoskeleton. Microtubule dynamics is essential for many vital cellular processes such as intracellular transport, metabolism, and cell division. We investigate the nonlinear dynamics of inhomogeneous microtubulin systems and the MT dynamics is found to be governed by a perturbed sine-Gordon equation. In the presence of various competing nonlinear inhomogeneities, it is shown that this nonlinear model can lead to the existence of kink and antikink solitons moving along MTs. We demonstrate kink–antikink pair collision in the framework of Hirota's bilinearization method. We conjecture that the collisions of the quanta of energy propagating in the form of kinks and antikinks may offer a new view of the mechanism of the retrograde and anterograde transport direction regulation of motor proteins in microtubulin systems.

Keywords: microtubules, solitons, solitary solutions, partial differential equations

PACS: 87.16.Ka, 03.75.Lm, 04.20.Jb, 02.60.Lj **DOI:** 10.1088/1674-1056/23/9/098703

1. Introduction

Microtubules (MTs) are important components of cytoskeletal structures,[1] which is in conjunction with actin and intermediate filaments, provide both static and dynamic frameworks that maintain cell structures. MTs belong to one of the three major classes of filaments, such a complex polymer network plays an essential role in many cellular functions such as separating chromosomes during mitosis, facilitating long-distance intracellular transport of both proteins and organelles, support the motor proteins to generate the force required for cell movement and changes in shapes, and acting as an important target for anticancer drugs.[2] Biological functions of MTs largely depend on their mechanical properties. More particularly, drugs that interfere with microtubule polymerization dynamics such as the tubulin-stabilising taxanes or the tubulin-destabilising vinca alkaloids have been proved to be more effective in the treatment of cancer.[3] MTs are also involved in specific myocardial cell functions, including regulation of contraction, ion channel function, receptor recycling, and sarcomere structure.[4–8] Interference with cellular microtubule dynamics results in mitotic arrest, prominent cytotoxicity and apparent angio-genesis inhibition, all of which can be translated into anticancer effects. Microtubules are essential to the assembly of the mitotic bipolar spindle which is responsible for proper chromosome segregation and cell division.

A microtubule is a hollow cylinder (Fig. 1) of about 25 nm in diameter. The interior of the cylinder (MTs) is likely to be filled with ordered water molecules, which implies the existence of electric dipoles and electric field.[9] The outer surface of MT is surrounded by oriented molecules of cytoplasmic water and enzymes.[10] Along the microtubule axis, tubulin heterodimers are joined end to end forming protofilaments, with alternating α and β subunits. MTs are composed of 12 to 17 protofilaments when self-assembled in vitro and almost exclusively of 13 protofilaments in vivo. These protofilaments are strongly bounded internally and are connected via weaker lateral bounds to form a sheet that is wrapped up into a tube in the nucleation process.[11] The wall of MT is made up of 13 identical protofilaments, each of which is a series of subunit proteins known as tubulin dimers. The dimers associated in a chain-like manner resulting in so called protofilaments. There are at least three tubulins associated with microtubules: α, β, and γ-tubulins. Each tubulin subunit is an 8-nm peanut-shaped dimer comprising α, β tubulin each consist of a single

*Project supported by the Serbian Ministry of Education and Sciences (Grant No. III45010), the URF from Periyar University, India, the research award of UGC, the major research project of NBHM, India, the Young Scientist Research Award of BRNS, India, the Junior Associateship of ICTP, Italy, and the Rajiv Gandhi National Fellowship of UGC.

†Corresponding author. E-mail: louiskavitha@yahoo.co.in

© 2014 Chinese Physical Society and IOP Publishing Ltd

polypeptide chain folded over on itself and is approximately 4 nm in diameter. Both α, β tubulin monomers have guanosine triphosphate (GTP) binding sites which play a critical role in the dynamics of microtubule formation. Monomers α- and β-tubulin assemble to form $\alpha\beta$-heterodimers each consisting of a single α-monomer and a single β-monomer. These heterodimers form the body of the microtubule as discussed in detail below. Monomers of γ-tubulin are bound at the ends of microtubule organizing centers (MTOCs), but not within microtubules themselves.

The basic building blocks of microtubules is the tubulin $\alpha\beta$-heterodimers. Dimers are polar in the sense that may have distinct α and β ends and so may attach to the growing microtubule with one of the possible orientation. It is well established that tubulin dimers attach to the growing microtubule with their β-monomer towards the distal end and their α-monomer towards the proximal end. The tubulin dimers polymerize (assembly) end to end in protofilaments. The protofilaments then bundle in hollow cylindrical filaments. The protofilaments arrange themselves in an imperfect helix with one turn of the helix containing 13 tubulin dimers each from a different protofilament.[9] As a rule one microtubule includes 13 rows of 8 nm×4 nm×4 nm tubulin dimers with a molecular weight of about 110 kDa. The microtubule structure is very likely nonlinear by itself. The binding energy of the tubulins in a heterodimer is very likely larger than that between two heterodimers. The dynamics of the microtubules is one of the most prominent features. The microtubules are capable of rapid polymerization and depolymerization which enables exchange of the subunits between soluble and polymer pools.

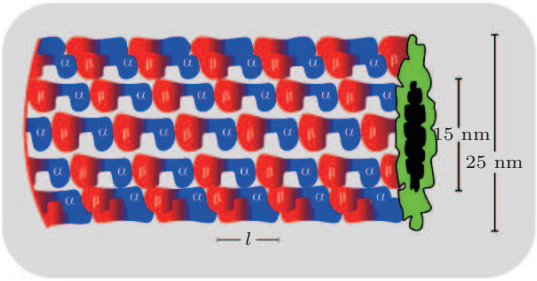


Fig. 1. (color online) Structural subunits of microtubules.

Several group of researchers put forward a hypothesis that this energy propagates along the MTs as a solitary wave. Chou *et al.*[12] showed that kinks and pulses are excited, for example by the energy freed in the GTP hydrolysis can propagate along MTs due to the coupling between the elastic states of the tubulin dimers. Satarić *et al.*[13] suggested that the nonlinear coupling between dielectric and elastic degrees of freedom of tubulin may give rise to kinklike excitations travelling along the MT protofilaments. The complex dynamics of MTs and other cytoskeletal elements play a key role in cell division, motility and determination of cell shape. Their elastic properties and interaction with the cell membrane are crucial in understanding cell morphology. Quantifying the mechanical properties of MTs is also necessary for explaining the elasticity of, for example sensory hair cells and sperm tails. Influence of various physical conditions such as temperature, or chemical agents for example drugs could introduce deformation in MTs. Previously performed experiments on mechanical properties of MTs reported in Ref. [14] involved bending or buckling MTs using optical tweezers,[15] hydrodynamic flow,[16] thermally induced vibrations or shape fluctuations,[17] and buckling in vesicles.[18] The physical quantity determining the behavior of MTs under this kind of deformation is the flexural rigidity or bending stiffness. On the other hand, structural studies involving electron microscopy[19] have shown that tubulin molecules are practically indistinguishable inside the single protofilament. Experimental observations[20] have found that motor protein kinesins can move along the parallel protofilaments of MTs without restrictions for them to jump between these protofilaments. Individual protofilaments are separated with grooves and linked to each other between β-tubulin molecules from adjacent protofilaments. Cryo-TEM studies of disassembling MTs[21] show that disassembly occurs by peeling apart the curved protofilament fragments at the ends of MTs. In MTs, inhomogeneity may also arise because of a local distortion that can be due to an attached associated protein or a structural discontinuity in the MT. Changing number of protofilaments, extra seams (discontinuity along a MT caused by the mismatch of the rows of tubulin dimers) and point dislocations have all been experimentally observed. There are strong arguments in favor of MTs being inhomogeneous and anisotropic, as well as composed of subunits that are more strongly bound in the longitudinal direction within protofilaments than laterally between protofilaments. The present paper, investigates the effect of various inhomogeneities of the protofilaments upon large oscillations of tubulin dimers. The paper is organized as follows. In Section 2, we formulate the bio-physical model for the inhomogeneous microtubulin systems and derive the dynamical equation in the form of a perturbed sine-Gordon equation. In Section 3, we employ the double-exponential function method aided with symbolic computation and the nonlinear dynamics of MTs under the influence of a variety of competing nonlinear inhomogeneities is explored. In Section 4, we demonstrate the collision scenario of kink–antikink pair in the framework of Hirota's bilinearization method and possible bio-physical significance of these kinks in the transport of motor proteins have also been discussed. The results are concluded in Section 5.

2. The model Hamiltonian and equations of motion

Within the cell, MTs assemble from individual monomers of the 55 kDa protein tubulin. It is assumed that each tubulin dimer has an associated electric dipole which can have only two possible orientations with respect to the longitudinal axis of the MT: When the dipole is pointing towards the distal end of the MT, the dimer is said to be in the "+1" state and when pointing in the opposite direction it is in the "−1" state. The angular displacement[13] of a dimer at a position n denoted as ϕ_n, which is a projection of the top of the dimer on the direction of protofilament (PF). The Hamiltonian for one PF is represented as follows:

$$H=\sum_n\left[\frac{I}{2}\dot{\phi}_n^2+\frac{kf_n}{2}\left(\phi_{n+1}-\phi_n\right)^2-qlE\cos\phi_n\right], \quad (1)$$

where the overdot represents the first derivative with respect to the time, I is the moment of inertia of the dimer, k represents the intra-dimer stiffness parameter and the integer n determines the position of the considered dimer in the PF.[22] The first term represents the kinetic energy of the dimer and the second term characterize the potential energy arises due to the chemical interaction between the neighbouring dimers. As an electrical dipole, a dimer in the presence of the intrinsic electric field E directed along the long axis of the MT cylinder, acquires the potential energy $U=-\boldsymbol{p}\cdot\boldsymbol{E}=-qlE\cos\phi_n$, where l is the distance between a center of positive and a center of negative charges and q is the excess charge within the dipole, with $q>0, E>0$.

In Fig. 2, the parameter f_n characterize the inhomogeneity in the angular displacement of dimers in one protofilament. If the stiffness parameter k is sufficiently large, then it is expected that large-amplitude long-wavelength excitations of the displacement field will be manifested by a slowly varying modulation of ϕ_n along the MT axis. Now for large oscillation using Hamiltonian (1), the Hamilton's equations of motion can be immediately written as

$$I\ddot{\phi}_n-k[f_n\phi_{n+1}+f_{n-1}\phi_{n-1}-\phi_n(f_n+f_{n-1})]+qlE\sin\phi_n=0, \quad (2)$$

which describes the dynamics of dimer at the discrete level ignoring the effect of viscosity. In addition, as the length of the PF is large when compared to the distance between the neighbouring dimers along the MT axis, we make a continuum approximation, which is valid in the long wavelength, low temperature limit, by introducing, the following Taylor series expansion for the functions

$$\phi_{n\pm1}=\phi(x,t)\pm R_0\left(\frac{\partial\phi}{\partial x}\right)+\frac{R_0^2}{2!}\left(\frac{\partial^2\phi}{\partial x^2}\right)\pm\cdots,$$
$$f_{n\pm1}=f(x,t)\pm R_0\left(\frac{\partial f}{\partial x}\right)+\frac{R_0^2}{2!}\left(\frac{\partial^2 f}{\partial x^2}\right)\pm\cdots,$$

where R_0 is the distance between the dimers. Assuming small inhomogeneity by choosing $f(x)=1+\varepsilon g(x)$, where ε is a parameter and $g(x)$ measures the strength of inhomogeneity. Recently, the study on local inhomogeneity arises since the hopping rate of one or several lattice sites of a PF is different from the hopping rates of the other sites of the PF. For example, a lattice site may be associated with a random quenched hopping rate[23] has received much attention.[23–25] Local inhomogeneities in MTs can be relevant to many biological processes such as energy transition of guanine triphosphate (GTP) hydrolysis,[26] cell growth,[27] excitations and inhibition of neurons,[28] and respiratory infection.[29] Using $\phi_{n\pm1}$ and $f_{n\pm1}$, equation (2), can be written down after making appropriate scaling and transformation as

$$\phi_{tt}-\phi_{xx}+\sin\phi=\varepsilon[g(x)\phi_{xx}+\Gamma g_x\phi_x], \quad (3)$$

where $\Gamma=\sqrt{kR_0^2/qlE}$. Equation (3) represents a perturbed sine-Gordon (sG) equation. When $\varepsilon=0$, equation (3) reduces to the completely integrable sine-Gordon equation which admits kink-type and antikink-type soliton solutions and it was originally solved to obtain N-soliton solutions using the most celebrated inverse scattering transform (IST) method, by Ablowitz and his co-workers.[30]

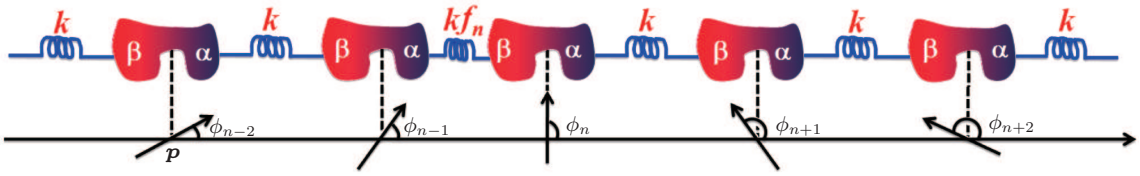


Fig. 2. (color online) Dimers in a protofilament with inhomogeneity.

Parallel arrayed MTs are interconnected by cross bridging proteins called microtubule-associated proteins. These interconnections, together with MTs are believed to be responsible for important cellular activities such as growth and division, which are very essential for the living state. Thus, MTs can be identified as oriented assemblies of dipoles. They are predicted to possess piezoelectric properties that may be quite important in their functions especially in the very inter-

esting assembly and disassembly behavior.[31,32] The attachment of a tubulin dimer at a growing MT end is accompanied by the hydrolysis of guanosine 5′-triphosphate (GTP), an energy-providing analog of adenosine 5′-triphosphate (ATP) which binds to polymerizing tubulin dimers. This chemical reaction takes place in the following way:

$$\mathrm{GTP}^{4-} + \mathrm{H_2O} \rightarrow \mathrm{GDP}^{3-} + \mathrm{HPO}_4^{2-} + \mathrm{H}^+ + \Delta E,$$

and under normal physiological conditions ΔE is the same for the hydrolysis of all 5′-triphosphate amounting to $\Delta E = 8.7$ kcal/mol.[33] One possible mechanism for the utilization of this form of energy is the production of coherent lattice vibrations as proposed by Fröhlich.[34] Also an interesting suggestion was made by Barnett[35] that filamentary cytoskeletal structures may operate much like information strings in analogy to semiconductor word processors. He also conjectured that MTs are indeed processing channels along which strings of information bits can move, transferring messages from place to place and in this context, it could be envisaged as playing the role of parallel-arrayed memory channels. It has also been suggested that if the stored mechanical energy is larger than the energy needed for the breakage of the bonds between the tubulin molecules, the surplus can be used to do mechanical work, for example, by coupling disassembly to the vesicle or chromosome movement.[36]

3. Implementation of the double exp-function method to microtubulin system

In order to better understand the microtubule dynamics as well as further to apply them in practical situations, it is important to seek the solitary wave solutions of the relevant model. Moreover, new solitary wave solutions may help to find new phenomena occurring in the microtubulin systems. Meantime powerful methods had been developed such as the Bäcklund transformation,[37] the Darboux transformation,[38] the inverse scattering transformation,[39] the bilinear method,[40] the generalized extended tangent hyperbolic function method,[41–46] the (G/G')-expansion method,[47] the sine-cosine method,[48] the homogeneous balance method,[49] the Riccati method,[50] the Jacobi elliptic function method[51–53] and the exp-function method,[54–56] etc to study the travelling wave solutions.

The exp-function method has been exploited for the determination of solitary wave solutions of many nonlinear differential equations and the double exp-function method was proposed in 2009 by Fu and Dai,[57] In addition, Ma *et al.*[58] constructed the multiple exp-function method to obtain multiple wave solutions, including one-soliton, two-soliton, and three-soliton type solutions to (3+1)-dimensional YTSF equation.

We try to obtain the soliton solution with double velocities and frequencies of the sine-Gordon equation which describes the dynamics of the microtubulin system. A large variety of physical, chemical, and biological phenomena are governed by nonlinear evolution equations. The analytical study of nonlinear partial differential equations is of great interest during the recent decades. These nonlinear phenomena are often related to nonlinear wave equations. In this section, we try to carry out the double exp-function method[57,59] to solve the perturbed sG equation. Now, we proceed the double exp-function method for Eq. (3) by choosing the following ansatz:

$$u(x,t) = \frac{\sum_{i=-m}^{n}\left[a_i \mathrm{e}^{\mathrm{i}\xi} + b_i \mathrm{e}^{\mathrm{i}\eta}\right]}{\sum_{j=-p}^{q}\left[c_j \mathrm{e}^{j\xi} + d_j \mathrm{e}^{j\eta}\right]}, \tag{4}$$

and introduce the following travelling wave solution $\phi = u(\xi,\eta)$, where ξ and η are the two travelling wave variables. Then the function ϕ is assumed to be rational functions of double exponential represented by $\exp(\xi)$ and $\exp(\eta)$. Here, $\xi = P_1 x + Q_1 t$, $\eta = P_2 x + Q_2 t$ and a_i, b_i, c_i, and d_i are the unknowns respectively. From a physical point of view, the study of propagation of nonlinear waves in microtubules is an exciting and important task. Therefore, we study the solitary wave solution of the microtubule using the above method. Substituting ϕ into the partial differential equation, we obtain the ordinary differential equation as

$$\begin{aligned}
&[Q_1^2 - (1+\varepsilon g)P_1^2]u_{\xi\xi}(\xi,\eta)\\
&+[Q_2^2 - (1+\varepsilon g)P_2^2]u_{\eta\eta}(\xi,\eta)\\
&+[2Q_1Q_2 - 2(1+\varepsilon g)P_1P_2]u_{\xi\eta}(\xi,\eta)\\
&-[\varepsilon\Gamma g_x P_1 + \varepsilon\Gamma P_2 + 1]u(\xi,\eta) - \frac{u(\xi,\eta)^3}{6} = 0.
\end{aligned} \tag{5}$$

Now substituting the series solution for u and by balancing the higher-order linear term with nonlinear term, we get $m = n$ and $p = q$. Let us choose for simplicity $m = n = p = q = 1$ and hence the solution for u can be written as

$$u(\xi,\eta) = \frac{a_{-1}\mathrm{e}^{-\xi} + a_1\mathrm{e}^{\xi} + a_0 + b_{-1}\mathrm{e}^{-\eta} + b_1\mathrm{e}^{\eta}}{c_{-1}\mathrm{e}^{-\xi} + c_1\mathrm{e}^{\xi} + b_0 + d_{-1}\mathrm{e}^{-\eta} + d_1\mathrm{e}^{\eta}}. \tag{6}$$

With the aid of symbolic package, we obtain the solitary wave solution of the dynamical equation governing the dynamics of microtubulin system

$$\begin{aligned}
u(\xi,\eta) = &\left[a_{-1}\mathrm{e}^{-\xi} + \left[\frac{c_1 b_0}{a_0}(-2\varepsilon\Gamma g_x P_1 - 2\varepsilon\Gamma P_2 - 2P_1P_2\right.\right.\\
&+P_1^2 + 2Q_1Q_2 + 2Q_2^2 - 2 - 2P_2^2\varepsilon g - 2P_2^2\\
&\left.\left.-2P_1P_2\varepsilon g + P_1^2\varepsilon g - Q_1^2)\right]\mathrm{e}^{\xi} + a_0 + b_{-1}\mathrm{e}^{-\eta}\right.\\
&+\left[\frac{1}{b_{-1}}(-2\varepsilon\Gamma P_2 b_0^2 - a_0^2 - 2P_2^2 b_0^2 + 12P_1^2 c_{-1}c_1\right.\\
&-2P_2^2\varepsilon g b_0^2 - 2b_0^2 - 4\varepsilon\Gamma g_x P_1 c_{-1}c_1 - 2\varepsilon\Gamma g_x P_1 b_0^2\\
&-12Q_1^2 c_{-1}c_1 - 4\varepsilon\Gamma P_2 c_{-1}c_1 + 12P_1^2\varepsilon g c_{-1}c_1\\
&+2Q_2^2 b_0^2 - 4c_{-1}c_1 + 4Q_2^2 c_{-1}c_1\\
&\left.\left.-4P_2^2 c_{-1}c_1 - 4P_2^2\varepsilon g c_{-1}c_1)\right]\mathrm{e}^{\eta}\right.\\
&\times[c_{-1}\mathrm{e}^{-\xi} + c_1\mathrm{e}^{\xi} + b_0 + d_{-1}\mathrm{e}^{-\eta} + d_1\mathrm{e}^{\eta}]^{-1},
\end{aligned} \tag{7}$$

where

$$d_1 = [A]\times[b_{-1}a_0qlE(P_1^2-2-3P_2^2+P_1^2\varepsilon g -6Q_1Q_2+3Q_2^2-3P_2^2\varepsilon g+6P_1P_2-Q_1^2 +6P_1P_2\varepsilon g-2\varepsilon\Gamma g_xP_1-2\varepsilon\Gamma P_2)]^{-1},$$

$$\begin{aligned}A = {} & -b_0(-2a_0^2qlE+P_1^2a_0^2qlE-Q_1^2a_0^2qlE\\ & +P_1^2\varepsilon ga_0^2qlE-2\varepsilon\Gamma P_2a_0^2qlE\\ & -2\varepsilon\Gamma g_xP_1a_0^2qlE+8c_{-1}c_1Q_1^2Q_2^2qlE\\ & -8c_{-1}c_1P_1^4\varepsilon gqlE-4c_{-1}c_1P_1^4\varepsilon^2g^2qlE\\ & -2c_{-1}c_1Q_2^2qlE+2c_{-1}c_1qlE-4c_{-1}c_1Q_1^4qlE\\ & -7c_{-1}c_1Q_1^2qlE-2c_{-1}c_1Q_1Q_2qlE\\ & +8c_{-1}c_1Q_1^3Q_2qlE-8c_{-1}c_1P_1^2Q_1Q_2qlE\\ & -4c_{-1}c_1P_1^4qlE+7c_{-1}c_1P_1^2\varepsilon gqlE\\ & -8c_{-1}c_1P_1^2\varepsilon gQ_2^2qlE-8c_{-1}c_1P_1^2Q_2^2qlE\\ & +7c_{-1}c_1P_1^2qlE+8c_{-1}c_1P_1^2Q_1^2qlE\\ & +8c_{-1}c_1P_1^2\varepsilon gQ_1^2qlE-8c_{-1}c_1P_1^2\varepsilon gQ_1Q_2qlE\\ & +2c_{-1}c_1\varepsilon^2kR_0^2g_x^2P_1^2-2c_{-1}c_1\varepsilon\Gamma g_xP_1Q_2^2qlE\\ & +7c_{-1}c_1\varepsilon^2\Gamma g_xP_1^3gqlE\\ & +4c_{-1}c_1\varepsilon\Gamma g_xP_1qlE+7c_{-1}c_1\varepsilon\Gamma g_xP_1^3qlE\\ & -2c_{-1}c_1\varepsilon\Gamma g_xP_1Q_1Q_2qlE\\ & -7c_{-1}c_1\varepsilon\Gamma g_xP_1Q_1^2qlE+2c_{-1}c_1\varepsilon^2\Gamma P_2^2P_1gqlE\\ & +8c_{-1}c_1P_1^3P_2qlE-7c_{-1}c_1\varepsilon\Gamma P_2Q_1^2qlE\\ & -8c_{-1}c_1Q_1^2P_2^2qlE-8c_{-1}c_1Q_1^2P_2^2\varepsilon gqlE\\ & -2c_{-1}c_1\varepsilon\Gamma P_2Q_1Q_2qlE\\ & +2c_{-1}c_1\varepsilon^2\Gamma P_2^3gqlE+2c_{-1}c_1P_1P_2qlE\\ & +7c_{-1}c_1P_1^2\varepsilon^2g\Gamma P_2qlE-8c_{-1}c_1Q_1^2P_1P_2qlE\\ & -8c_{-1}c_1Q_1^2P_1P_2\varepsilon gqlE\\ & +4c_{-1}c_1\varepsilon^2kR_0^2g_xP_1P_2+2c_{-1}c_1\varepsilon\Gamma g_xP_1^2P_2qlE\\ & +2c_{-1}c_1\varepsilon^2\Gamma g_xP_1P_2^2gqlE\\ & +16c_{-1}c_1P_1^3\varepsilon gP_2qlE+8c_{-1}c_1P_1^2\varepsilon^2g^2P_2^2qlE\\ & +16c_{-1}c_1P_1^2\varepsilon gP_2^2qlE+8c_{-1}c_1\\ & \times P_1^3\varepsilon^2g^2P_2qlE+2c_{-1}c_1\varepsilon\Gamma P_2^2P_1qlE\\ & +7c_{-1}c_1\varepsilon\Gamma P_2P_1^2qlE+8c_{-1}c_1P_1^2P_2^2qlE\\ & +2c_{-1}c_1P_1P_2\varepsilon gqlE+2c_{-1}c_1\varepsilon^2kR_0^2P_2^2\\ & +4c_{-1}c_1\varepsilon\Gamma P_2qlE+2c_{-1}c_1P_2^2\varepsilon gqlE\\ & +2c_{-1}c_1P_2^2qlE-2c_{-1}c_1\varepsilon\Gamma P_2Q_2^2qlE\\ & +2c_{-1}c_1\varepsilon\Gamma P_2^3qlE+2c_{-1}c_1\varepsilon^2\Gamma g_xP_1^2P_2gqlE\\ & +2c_{-1}c_1\varepsilon\Gamma g_xP_1P_2^2qlE).\end{aligned}$$

3.1. Dynamics of microtubules with various inhomogeneities

In order to analyze the effect of a variety of competing nonlinear inhomogeneities that may occur in general in tubulin systems, we assume the function $g(x)$ which takes the form of (i) linear inhomogeneity, (ii) quadratic inhomogeneity, (iii) localized inhomogeneity in the form of tangent hyperbolic inhomogeneity, and (iv) exponential inhomogeneity and discuss the nature of evolution of solutions under each case.

When the inhomogeneity varies in the form of $g(x) = Bx + C$, where B and C are arbitrary constants. The solution represented by Eq. (7) for the case of linear inhomogeneity is plotted in Figs. 3(a)–3(c) and the solution assumes the form of anti-kinkon for the parametric values $q = 6\times10^{-18}$ C, $l = 8\times10^{-9}$ m, $E = 10^5$ V·m^{-1}, $c_1 = 0.1\times10^{-3}$, $b_0 = 0.1\times10^{-9}$, $\varepsilon = 0.5$, $R_0 = 10^{-8}$ m, $P_1 = 0.2$, $P_2 = 0.3$, $Q_1 = 0.2$, $Q_2 = 0.5$, $a_0 = 6\times10^{-9}$, $c_{-1} = 0.2$, $b_{-1} = 0.02$, $a_{-1} = 0.1$, $d_{-1} = 0.2$, $C = 2$, and $B = 0.01$. Further increase in B, introduces a more steepened ramp in the anti-kinkon and the higher end of the anti-kinkon hightens more and more with the increased amplitude, as depicted in Fig. 3(c). Having known the effect of linear inhomogeneity on the anti-kinkon governing the dynamics of tubulin systems, we try to analyze the effect of nonlinear inhomogeneity. We assume the function that takes the form of a quadratic nonlinear function, i.e. $g(x) = Ax^2 + Bx + C$, where A, B, and C are arbitrary constants. We have plotted Eq. (7) for the case of quadratic inhomogeneity, by choosing the parameters $q = 6\times10^{-18}$ C, $l = 8\times10^{-9}$ m, $E = 10^5$ V·m^{-1}, $k = 1$, $c_1 = 0.1$, $b_0 = 10^{-14}$, $\varepsilon = 0.5$, $R_0 = 10^{-8}$ m, $P_1 = 0.1$, $P_2 = 10^{-18}$, $Q_1 = 0.1$, $Q_2 = 0.5$, $a_0 = 1$, $c_{-1} = 0.1$, $b_{-1} = 0.002$, $a_{-1} = 0.1$, and $d_{-1} = 0.2$ in Figs. 3(d)–3(f). When the value of the quadratic co-efficient is increased, the well defined anti-kinkon profile is slowly transformed into a double anti-kinkon, when $A = 1$, as shown in the snapshots of the Figs. 3(d)–3(f). Next, we consider another type of inhomogeneity, namely a localized inhomogeneity which is taken in the form of a tangent hyperbolic function. In Figs. 4(a)–4(c), we have plotted Eq. (7), for the case of localized tangent inhomogeneity $g(x) = \alpha\tanh(x)$, for the choices of parameters $q = 6\times10^{-18}$ C, $l = 8\times10^{-9}$ m, $E = 10^5$ V·m^{-1}, $k = 1$, $c_1 = 0.001$, $b_0 = 1\times10^{-7}$, $\varepsilon = 0.5$, $R_0 = 10^{-8}$ m, $P_1 = 0.2$, $P_2 = 0.3$, $Q_1 = 0.2$, $Q_2 = 0.5$, $a_0 = 6\times10^{-9}$, $c_{-1} = 0.2$, $b_{-1} = 0.02$, $a_{-1} = 0.1$, and $d_{-1} = 0.2$. When the strength of localized inhomogeneity is lower, i.e., $\alpha = 0.05$, the solution assumes a form of more stable and robust soliton. When the value of α is increased, a peak is developed at the center of the solitonic hump as shown in the snapshots depicted in Figs. 4(d)–4(f). The amplitude of the sharp peak is increased for further increase in α. Surprisingly, when the inhomogeneity assumes the form of a exponential function $g(x) = \delta\exp(\delta x)$, the plot for Eq. (7), depicts a cleavaged double-kink with differing amplitude as shown in Figs. 4(d)–4(f)) revealing the mysterious nature of the solution when the strength of the inhomogeneity is increased. When the value of δ is increased, one of the cleavaged double-kink increases in amplitude and once both of them having the same amplitude, the other one starts to shorten gradually, as displayed in Figs. 4(a)–4(c). When $\delta = 10$, more surprisingly, the other

part of the cleavaged double-kink vanishes, leaving its counterpart intact. It is well known that extra energy is required in order to create a kink, since kinks are not solutions of the equation of motion with the lowest energy. This extra energy can be produced, for example, during the hydrolysis of ATP or GTP. From the above results, one can conclude that a unique kink-like excitation exists in MTs which may propagate with a unique velocity that, in the given range of parameters, is proportional to the type of inhomogeneity present in the MTs. In addition the kink-like domain walls can be viewed as bits of information propagating along MTs.[13] Due to the coupling between dielectric and elastic degrees of freedom of tubulin, this information can be coupled to mechanical events. For example, such kinks may be involved in the movement of motor proteins.

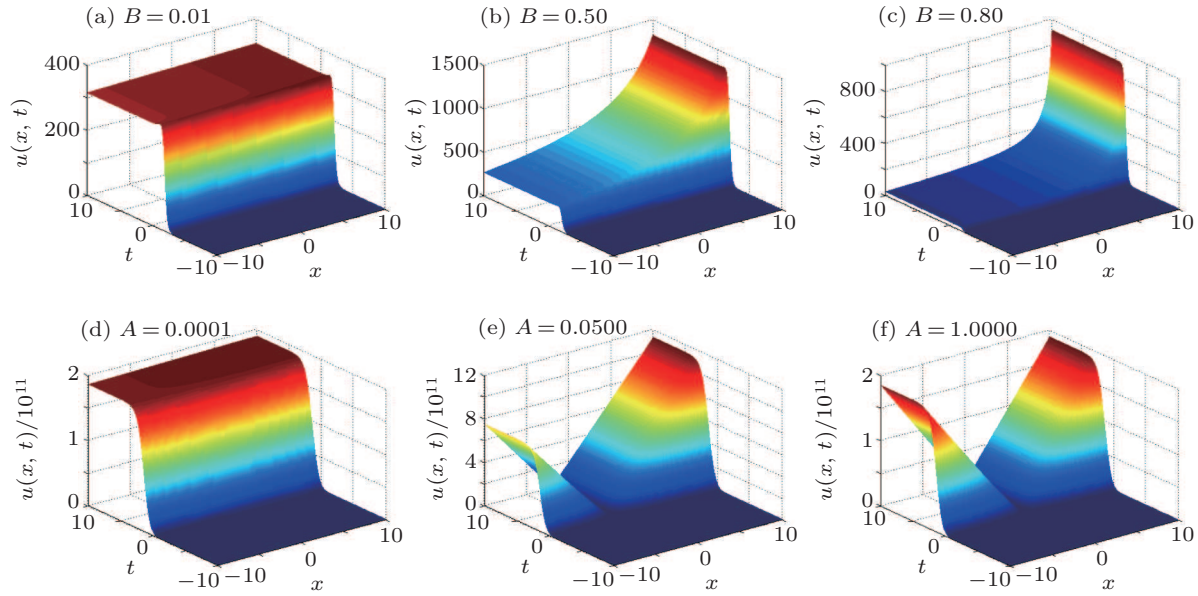


Fig. 3. (color online) (a)–(c) Amplitude variation of antikink-soliton under the influence of linear inhomogeneity for various values of parameters $q = 6 \times 10^{-18}$ C, $l = 8 \times 10^{-9}$ m, $E = 10^5$ V·m^{-1}, $c_1 = 0.1 \times 10^{-3}$, $b_0 = 0.1 \times 10^{-9}$, $\varepsilon = 0.5$, $R_0 = 10^{-8}$ m, $P_1 = 0.2$, $P_2 = 0.3$, $Q_1 = 0.2$, $Q_2 = 0.5$, $a_0 = 6 \times 10^{-9}$, $c_{-1} = 0.2$, $b_{-1} = 0.02$, $a_{-1} = 0.1$, $d_{-1} = 0.2$, and $C = 2$. (d)–(f) Distorted antikink profile under the influence of quadratic inhomogeneity for various values of parameters $c_1 = 0.1$, $b_0 = 10^{-14}$, $P_1 = 0.1$, $P_2 = 10^{-18}$, $Q_1 = 0.1$, $Q_2 = 0.5$, $a_0 = 1$, $c_{-1} = 0.1$, and $b_{-1} = 0.002$.

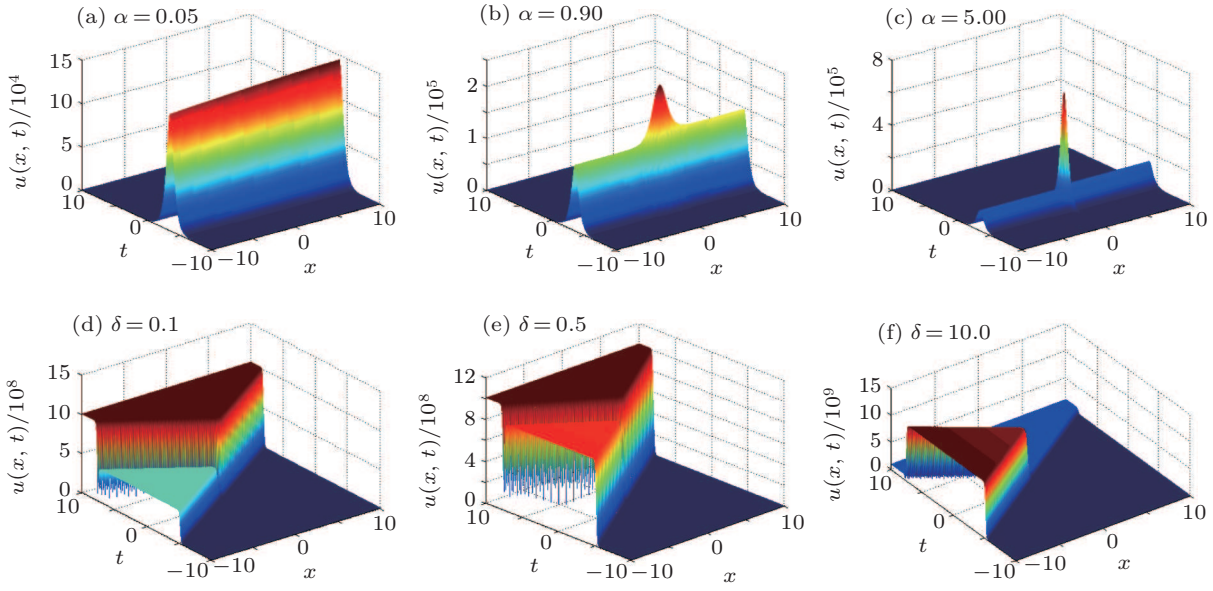


Fig. 4. (color online) (a)–(c) Snapshots of soliton with localized inhomogeneity for various values of parameters $q = 6 \times 10^{-18}$ C, $l = 8 \times 10^{-9}$ m, $E = 10^5$ V·m^{-1}, $k = 1$, $c_1 = 0.001$, $b_0 = 1 \times 10^{-7}$, $\varepsilon = 0.5$, $R_0 = 10^{-8}$ m, $P_1 = 0.2$, $P_2 = 0.3$, $Q_1 = 0.2$, $Q_2 = 0.5$, $a_0 = 6 \times 10^{-9}$, $c_{-1} = 0.2$, $b_{-1} = 0.02$, $a_{-1} = 0.1$, and $d_{-1} = 0.2$. (d)–(f) Snapshots of cleavaged antikink-soliton with exponential inhomogeneity for various values of parameters $c_1 = 0.0001$, $b_0 = 0.1$, $\varepsilon = 0.5$, $P_2 = 0.4$, $Q_1 = 2$, $Q_2 = 5$, $a_0 = 4 \times 10^{-9}$, $b_{-1} = 0.2$, and $d_{-1} = 2 \times 10^{-10}$.

4. Hirota bilinearization and kink-collision in tubulin systems

In the present section, we perform a systematic analysis on the collision behavior of kinkons and examine the shape-changing collisions through Hirota bilinearization procedure.[60] Hirota developed a systematic method to obtain solitary wave solutions of nonlinear PDEs and this method has profound impact on the soliton theory. This method is found to be consistent and applicable to large class of nonlinear evolution equations that also include integro-differential equations. The essence of this method is to construct the N-soliton solution for a given nonlinear evolution equation and able to identify the collision property of the nonlinear equation associated with the solitons. The fundamental idea is to use a dependent variable transformation to convert nonlinear PDE into a new evolution equation where the new dependent variable appears bilinearly.[61] The tedious tasks involved is that it requires an enormous effort in solving the algebraic equations. However, we briefly outline the procedure to demonstrate the collision of kinkon solutions of the perturbed inhomogeneous sG equation. By performing the bilinearizing transformation $\phi = 4\tan^{-1}(G/F)$, where G is a complex function while F is the real valued function of x and t. Substituting the above transformation in Eq. (3) reduces to

$$\begin{aligned}
&\Big(D_t^2 - (1+\varepsilon g)\frac{kR_0^2}{2I}D_x^2 + \frac{qlE}{I}\Big)(GF) = 0,\\
&D_t^2(GG) - D_t^2(FF) + (1+\varepsilon g)\frac{kR_0^2}{2I}\Big(D_x^2(FF) - D_x^2(GG)\Big) = 0,\\
&D_x(GF) = 0, \qquad (8)
\end{aligned}$$

which can be solved by introducing the following power series expansions for $G = \varepsilon_1 G_1 + \varepsilon_1^3 G_3 + \cdots$, and $F = 1 + \varepsilon_1^2 F_2 + \varepsilon_1^4 F_4 + \cdots$, where ε_1 is the formal expansion parameter.

4.1. Multisoliton solutions

In this section, we try to elucidate the one and two soliton solutions for the microtubulin systems governed by the perturbed sG equation by solving the respective Hirota bilinearizing operators Eq. (8).

4.1.1. One-soliton solution

The one-soliton solution of Eq. (3) can be written by restricting the power series of F and G to the lowest order in ε_1. Then by solving the resulting set of equations recursively, one can write down the explicit form of one soliton solutions using F and G as

$$\phi = 4\tan^{-1}\Big(\frac{G}{F}\Big) = 4\tan^{-1}\Big(\frac{\varepsilon_1 G_1}{1+\varepsilon_1^2 F_2}\Big), \qquad (9)$$

where $\varepsilon_1 = 1$, $G_1 = \gamma_1 \mathrm{e}^{\theta_1}$, $\theta_1 = K_1 x + \omega_1 t + \theta_1(0)$,

$$\omega_1 = \sqrt{\Big((1+\varepsilon g)\frac{kR_0^2}{2I}\Big)K_1^2 - \frac{qlE}{I}}, \quad g = Bx + C, \quad F_2 = 0.$$

4.1.2. Two-soliton solution

The two-soliton solutions can be obtained by terminating the power series expansion of F and G upto the order of ε_1. By substituting the above expansions into the bilinear equation (8) and solving the set of equations, we get F_2, G_3, and F_4 respectively. Using that, we write down the explicit form of the two soliton solution for the microtubulin system as

$$\phi = 4\tan^{-1}\Big(\frac{G}{F}\Big) = 4\tan^{-1}\Big(\frac{\varepsilon_1 G_1 + \varepsilon_1^3 G_3}{1+\varepsilon_1^2 F_2 + \varepsilon_1^4 F_4}\Big), \qquad (10)$$

where

$$\begin{aligned}
\varepsilon_1 &= 1, \quad G_1 = \gamma_1 \mathrm{e}^{\theta_1} + \gamma_2 \mathrm{e}^{\theta_2},\\
\theta_1 &= K_1 x + \omega_1 t + \theta_1(0),\\
\theta_2 &= K_2 x + \omega_2 t + \theta_2(0),\\
F_2 &= -\gamma_1\gamma_2 \mathrm{e}^{\theta_1+\theta_2},\\
G_3 &= \Big(\frac{-\gamma_1^2\gamma_2 K_2}{2K_1+K_2}\Big)\mathrm{e}^{2\theta_1+\theta_2} + \Big(\frac{-\gamma_1\gamma_2^2 K_1}{2K_2+K_1}\Big)\mathrm{e}^{2\theta_2+\theta_1},\\
F_4 &= \frac{(-\gamma_1^3\gamma_2 K_2)\Big[K_1K_2\Big((1+\varepsilon g)\frac{kR_0^2}{2I}\Big) - \omega_1\omega_2 - \frac{qlE}{I}\Big]}{(2K_1+K_2)\Big[6K_1K_2\Big((1+\varepsilon g)\frac{kR_0^2}{2I}\Big) + 18 - 6\omega_1\omega_2\Big]}\mathrm{e}^{3\theta_1+\theta_2}\\
&\quad - \Big(\frac{4\gamma_1^2\gamma_2^2 K_2}{2K_1+K_2} + \frac{4\gamma_1^2\gamma_2^2 K_1}{2K_2+K_1}\Big)\\
&\quad \times \frac{\mathrm{e}^{2\theta_1+2\theta_2}}{8\Big[K_1K_2\Big((1+\varepsilon g)\frac{kR_0^2}{2I}\Big) + \frac{qlE}{I} - 8\omega_1\omega_2\Big]} - \frac{\gamma_1\gamma_2^3 K_1}{2K_2+K_1}\\
&\quad \times \Bigg\{\frac{K_1K_2\Big[(1+\varepsilon g)\frac{kR_0^2}{2I}\Big] - \omega_1\omega_2 - \frac{qlE}{I}}{6K_1K_2\Big[(1+\varepsilon g)\frac{kR_0^2}{2I}\Big] + 10 - 6\omega_1\omega_2}\Bigg\}\mathrm{e}^{3\theta_2+\theta_1}.
\end{aligned}$$

4.1.3. Three-soliton solution

The three-soliton solutions can be obtained by terminating the power series expansion upto the order of ε_5 given by $G = \varepsilon_1 G_1 + \varepsilon_1^3 G_3 + \varepsilon_1^5 G_5$, $F = 1 + \varepsilon_1^2 F_2 + \varepsilon_1^4 F_4 + \varepsilon_1^6 F_6$. By substituting the above expansions into the bilinear equation (8) and solving the set of equations, we get G_3, G_5, F_2, F_4, and F_6 respectively. Using that, we write down the explicit form of the three soliton solution for the microtubulin system as

$$\phi = 4\tan^{-1}\Big(\frac{G}{F}\Big) = 4\tan^{-1}\Big(\frac{\varepsilon_1 G_1 + \varepsilon_1^3 G_3 + \varepsilon_1^5 G_5}{1+\varepsilon_1^2 F_2 + \varepsilon_1^4 F_4 + \varepsilon_1^6 F_6}\Big), \qquad (11)$$

where

$$\begin{aligned}
\varepsilon_1 &= 1, \quad G_1 = \gamma_1 \mathrm{e}^{\theta_1} + \gamma_2 \mathrm{e}^{\theta_2} + \gamma_3 \mathrm{e}^{\theta_3},\\
\theta_1 &= K_1 x + \omega_1 t + \theta_1(0), \quad \theta_2 = K_2 x + \omega_2 t + \theta_2(0),\\
\theta_3 &= K_3 x + \omega_3 t + \theta_3(0),\\
G_1 &= \gamma_1 \mathrm{e}^{\theta_1} + \gamma_2 \mathrm{e}^{\theta_2} + \gamma_3 e\, \mathrm{e}^{\theta_3}, \quad G_3 = \mathrm{e}^{\theta_1+\theta_2+\theta_3+b_{11}},\\
G_5 &= (\mathrm{e}^{2\theta_1+2\theta_2+\theta_3+d_{11}} + \mathrm{e}^{2\theta_2+2\theta_3+\theta_1+d_{22}}\\
&\quad + \mathrm{e}^{2\theta_1+2\theta_3+\theta_2+d_{33}} + \mathrm{e}^{3\theta_1+\theta_2+\theta_3+d_{44}}\\
&\quad + \mathrm{e}^{3\theta_2+\theta_1+\theta_3+d_{55}} + \mathrm{e}^{3\theta_3+\theta_1+\theta_2+d_{66}}),
\end{aligned}$$

$$
\begin{aligned}
F_2 &= (\mathrm{e}^{\theta_1+\theta_2+a_{11}} + \mathrm{e}^{\theta_1+\theta_3+a_{22}} + \mathrm{e}^{\theta_2+\theta_3+a_{33}}),\\
F_4 &= (\mathrm{e}^{2\theta_1+\theta_2+\theta_3+c_{11}} + \mathrm{e}^{2\theta_2+\theta_1+\theta_3+c_{22}} + \mathrm{e}^{2\theta_3+\theta_1+\theta_2+c_{33}}),\\
F_6 &= (\mathrm{e}^{3\theta_1+2\theta_2+\theta_3+h_{11}} + \mathrm{e}^{2\theta_1+2\theta_2+2\theta_3+h_{22}}\\
&\quad + \mathrm{e}^{3\theta_1+2\theta_3+\theta_2+h_{33}} + \mathrm{e}^{4\theta_1+\theta_2+\theta_3+h_{44}}\\
&\quad + \mathrm{e}^{3\theta_2+2\theta_1+\theta_3+h_{55}} + \mathrm{e}^{3\theta_3+2\theta_1+\theta_2+h_{66}}\\
&\quad + \mathrm{e}^{3\theta_2+2\theta_3+\theta_1+h_{77}} + \mathrm{e}^{4\theta_2+\theta_1+\theta_3+h_{88}}\\
&\quad + \mathrm{e}^{3\theta_3+2\theta_2+\theta_1+h_{99}} + \mathrm{e}^{4\theta_3+\theta_1+\theta_2+h_{10}}),\\
h_{11} &= \{\gamma_1[(1+A)(K_1+2K_2+K_3)^2-(\omega_1+2\omega_2+\omega_3)^2]\mathrm{e}^{d_{11}}\\
&\quad + \gamma_2[(1+A)(3K_1+K_3)^2-(3\omega_1+\omega_3)^2]\mathrm{e}^{d_{44}}\\
&\quad + [(\omega_1+\omega_3)^2-(1+A)(K_1+K_3)^2]\mathrm{e}^{c_{11}+a_{11}}\}\\
&\quad \times[(1+A)(3K_1+2K_2+K_3)^2\\
&\quad -(3\omega_1+2\omega_2+\omega_3)^2]^{-1},\\
h_{22} &= \{\gamma_1[(1+A)(2K_2+2K_3)^2-(\omega_2+2\omega_3)^2]\mathrm{e}^{d_{22}}\\
&\quad + \gamma_2[(1+A)(2K_1+2K_3)^2-(2\omega_1+2\omega_3)^2]\mathrm{e}^{d_{33}}\\
&\quad + \gamma_3[-(\omega_1+2\omega_2)^2+(1+A)(2K_1+2K_2)^2]\mathrm{e}^{d_{11}}\}\\
&\quad \times[(1+A)(2K_2+2K_3+2K_1)^2-(2\omega_2+2\omega_3+2\omega_1)^2]^{-1},\\
h_{33} &= \{\gamma_1[(1+A)(K_1+K_2+2K_3)^2-(\omega_1+\omega_2+2\omega_3)^2]\mathrm{e}^{d_{33}}\\
&\quad + \gamma_3[(1+A)(3K_1+K_2)^2-(3\omega_1+\omega_2)^2]\mathrm{e}^{d_{44}}\\
&\quad + [(\omega_1+\omega_2)^2-(1+A)(K_1+K_2)^2]\mathrm{e}^{c_{11}+a_{22}}\}\\
&\quad \times[(1+A)(3K_1+2K_3+K_2)^2-(3\omega_1+2\omega_3+\omega_2)^2]^{-1},\\
h_{44} &= \frac{\gamma_1[(1+A)(2K_1+K_2+K_3)^2-(2\omega_1+\omega_2+\omega_3)^2]\mathrm{e}^{d_{44}}}{(1+A)(4K_1+K_2+K_3)^2-(4\omega_1+\omega_2+\omega_3)^2)},\\
h_{55} &= \{\gamma_1[(1+A)(3K_2+K_3)^2-(3\omega_2+\omega_3)^2]\mathrm{e}^{d_{55}}\\
&\quad + \gamma_2\Big(1+A)(2K_1+K_2+K_3)^2-(2\omega_1+\omega_2+\omega_3)^2]\mathrm{e}^{d_{11}}\\
&\quad + [(\omega_2+\omega_3)^2-(1+A)(K_2+K_3)^2]\mathrm{e}^{c_{22}+a_{11}}\}\\
&\quad \times[(1+A)(3K_2+2K_1+K_3)^2-(3\omega_2+2\omega_1+\omega_3)^2]^{-1},\\
h_{66} &= \{\gamma_1[(1+A)(3K_3+K_2)^2-(3\omega_3+\omega_2)^2]\mathrm{e}^{d_{66}}\\
&\quad + \gamma_3[(1+A)(2K_1+K_2+K_3)^2-(2\omega_1+\omega_2+\omega_3)^2]\mathrm{e}^{d_{33}}\\
&\quad + [(\omega_3+\omega_2)^2-(1+A)(K_3+K_2)^2]\mathrm{e}^{c_{33}+a_{22}}\}\\
&\quad \times[(1+A)(3K_3+2K_1+K_2)^2-(3\omega_3+2\omega_1+\omega_2)^2]^{-1},\\
h_{77} &= \{\gamma_2[(1+A)(K_1+K_2+2K_3)^2-(\omega_1+\omega_2+2\omega_3)^2]\mathrm{e}^{d_{22}}\\
&\quad + \gamma_3[(1+A)(3K_2+K_3)^2-(3\omega_2+\omega_1)^2]\mathrm{e}^{d_{55}}\\
&\quad + [(\omega_1+\omega_2)^2-(1+A)(K_1+K_2)^2]\mathrm{e}^{c_{22}+a_{33}}\}\\
&\quad \times[(1+A)(3K_2+2K_3+K_1)^2-(3\omega_2+2\omega_3+\omega_1)^2]^{-1},\\
h_{88} &= \frac{\gamma_2[(1+A)(2K_2+K_1+K_3)^2-(2\omega_2+\omega_1+\omega_3)^2]\mathrm{e}^{d_{55}}}{(1+A)(4K_2+K_1+K_3)^2-(4\omega_2+\omega_1+\omega_3)^2},\\
h_{99} &= \{\gamma_2[(1+A)(K_1+3K_3)^2-(\omega_1+3\omega_3)^2]\mathrm{e}^{d_{66}}\\
&\quad + \gamma_3[(1+A)(K_1+2K_2+K_3)^2-(\omega_1+2\omega_2+\omega_3)^2]\mathrm{e}^{d_{22}}\\
&\quad + [(\omega_1+\omega_3)^2-(1+A)(K_1+K_3)^2]\mathrm{e}^{c_{33}+a_{33}}\}\\
&\quad \times[(1+A)(3K_3+2K_2+K_1)^2-(3\omega_3+2\omega_2+\omega_1)^2]^{-1},\\
h_{10} &= \frac{\gamma_3[(1+A)(K_1+K_2+2K_3)^2-(\omega_1+\omega_2+2\omega_3)^2]\mathrm{e}^{d_{66}}}{(1+A)(4K_3+K_1+K_2)^2-(4\omega_3+\omega_1+\omega_2)^2},\\
d_{11} &= \frac{\mathrm{e}^{b_{11}+a_{11}}+\gamma_1\mathrm{e}^{c_{22}}+\mathrm{e}^{c_{11}}}{(2\omega_1+2\omega_2+\omega_3)^2-(2K_1+2K_2+K_3)^2+(qlE/I)},\\
d_{22} &= \frac{\mathrm{e}^{b_{11}+a_{33}}+\gamma_2\mathrm{e}^{c_{33}}+\gamma_3\mathrm{e}^{c_{22}}}{(2\omega_2+2\omega_3+\omega_1)^2-(2K_2+2K_3+K_1)^2+(qlEI)},\\
d_{33} &= \frac{\mathrm{e}^{b_{11}+a_{22}}+\gamma_1\mathrm{e}^{c_{33}}+\gamma_3\mathrm{e}^{c_{11}}}{(2\omega_1+2\omega_3+\omega_2)^2-(2K_1+2K_3+K_2)^2+(qlE/I)},\\
d_{44} &= \frac{\gamma_1\mathrm{e}^{c_{11}}}{(3\omega_1+\omega_2+\omega_3)^2-(3K_1+K_2+K_3)^2+(qlE/I)},\\
d_{55} &= \gamma_2\mathrm{e}^{c_{22}}\Bigg[(3\omega_2+\omega_1+\omega_3)^2-(1+A)\\
&\quad \times(3K_2+K_1+K_3)^2+\left(\frac{qlE}{I}\right)\Bigg]^{-1},\\
d_{66} &= \gamma_3\mathrm{e}^{c_{33}}\Bigg[(3\omega_3+\omega_1+\omega_2)^2-(1+A)\\
&\quad \times(3K_3+K_1+K_2)^2+\left(\frac{qlE}{I}\right)\Bigg]^{-1},
\end{aligned}
$$

$$
\begin{aligned}
c_{11} &= \frac{\gamma_1[(1+A)(K_2+K_3)^2-(\omega_2+\omega_3)^2]\mathrm{e}^{b_{11}}+[(\omega_3-\omega_2)^2-(1+A)(K_3-K_2)^2]\mathrm{e}^{a_{11}+a_{22}}}{(1+A)(2K_1+K_2+K_3)^2-(2\omega_1+\omega_2+\omega_3)^2},\\
c_{22} &= \frac{\gamma_2[(1+A)(K_1+K_3)^2-(\omega_1+\omega_3)^2]\mathrm{e}^{b_{11}}+[(\omega_3-\omega_1)^2-(1+A)(K_3-K_1)^2]\mathrm{e}^{a_{11}+a_{33}}}{(1+A)(2K_2+K_1+K_3)^2-(2\omega_2+\omega_1+\omega_3)^2},\\
c_{33} &= \frac{\gamma_3[(1+A)(K_1+K_2)^2-(\omega_1+\omega_2)^2]\mathrm{e}^{b_{11}}+[(\omega_2-\omega_1)^2-(1+A)(K_2-K_1)^2]\mathrm{e}^{a_{22}+a_{33}}}{(1+A)(2K_3+K_1+K_2)^2-(2\omega_3+\omega_1+\omega_2)^2},\\
b_{11} &= \gamma_1[2\omega_1(\omega_2+\omega_3)-(\omega_2+\omega_3)^2-2(1+A)K_1(K_2+K_3)+(1+A)(K_2+K_3)^2]\mathrm{e}^{a_{33}}\\
&\quad +\gamma_2[2\omega_2(\omega_1+\omega_3)-(\omega_1+\omega_3)^2-2(1+A)K_2(K_1+K_3)+(1+A)(K_1+K_3)^2]\mathrm{e}^{a_{22}}\\
&\quad +\gamma_3[2\omega_3(\omega_1+\omega_2)-(\omega_1+\omega_2)^2-2(1+A)K_3(K_1+K_2)+(1+A)(K_1+K_2)^2]\mathrm{e}^{a_{11}},\\
a_{11} &= \frac{\gamma_1\gamma_2[(1+A)(\frac{kR_0^2}{I})(K_1-K_2)^2-(\omega_1-\omega_2)^2]}{(1+A)(\frac{kR_0^2}{I})(K_1+K_2)^2-(\omega_1+\omega_2)^2},\quad
a_{22} = \frac{\gamma_1\gamma_3[(1+A)(\frac{kR_0^2}{I})(K_1-K_3)^2-(\omega_1-\omega_3)^2]}{(1+A)(\frac{kR_0^2}{I})(K_1+K_3)^2-(\omega_1+\omega_3)^2},\\
a_{33} &= \frac{\gamma_2\gamma_3[(1+A)(\frac{kR_0^2}{I})(K_2-K_3)^2-(\omega_2-\omega_3)^2]}{(1+A)(\frac{kR_0^2}{I})(K_2+K_3)^2-(\omega_2+\omega_3)^2}.
\end{aligned}
$$

In addition, one can proceed as before for the general case, with the choice

$$\phi(x,t) = 4\tan^{-1}\left(\frac{G_i}{F_i}\right), \quad i = 1,2,3,\ldots,N, \tag{12}$$

and N-soliton solutions can be obtained for finite N, where $N \geq 1$.

4.2. Collision dynamics of kink-solitons in protofilament

In this section, we demonstrate the collision between kink and antikink solitons in the framework of Hirota's bilinearization method. One of the most exciting phenomena associated with the kinkons is their collision. In linear media, a localized wave packet propagates through another wave packet, completely unaffected by its presence. In contrast, in nonlinear media such as microtubulin systems, these kinkons can exchange energy, bounce off each other, spiral around each other, and display many other exciting interaction-associated phenomena. Figure 5 portrays the snapshots of kink–antikink collisions as a function of linear inhomogeneity $g(x) = Bx + C$. From Fig. 5(a), we could observe that the incoming pair of kink and antikink copropagate towards the collision point for the value of $B = 2.1$ and figure 6(a) depicts a more explanatory collision scenario at two typical moments at $t = -10$ and $t = 10$ representing before and after inelastic collision respectively. As a result of an inelastic collision, there is an abrupt exchange of energy among the dimers of MTs and the kink–antikink pair emerges with decrease of energies as depicted in Fig. 6(a). Surprisingly, when the value of the coefficient of linear inhomogeneity $B = 2.2$, the same scenario of decrease in energies of kink–antikink pair happens as a result of an inelastic collision as depicted in Fig. 6(b) and in this case the area of the central collision plateau is significantly reduced, as manifested in Fig. 5(b). When $B = 2.3$, the energy of the antikink remains invariant as a result of collision whereas the energy of the kink is decreased, leaving the area of the central collision plateau subsequently reduced as shown in Figs. 5(c) and 6(c) respectively. In what follows, we briefly analyze the effect of the presence of nonlinear inhomogeneity in the form of a quadratic function $g(x) = Ax^2 + Bx + C$ on the energy sharing mechanism between kink–antikink pair as a result of collision.

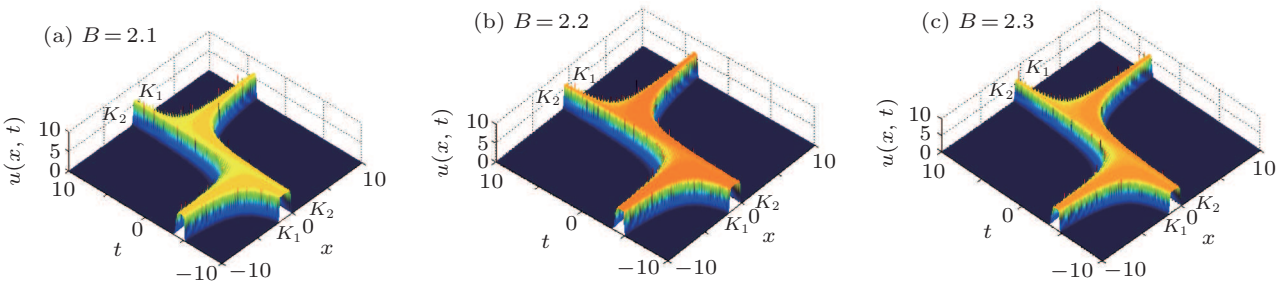


Fig. 5. (color online) Snapshots of inelastic collision between kink–antikink pair for various values of parameters $\theta_1(0) = 0.1 + i$, $\theta_2(0) = 0.1 - i$, $k = 2 \times 10^{-16}$, $l = 8 \times 10^{-9}$ m, $R_0 = 10^{-8}$ m, $I = 1 \times 10^{-39}$ kg·m^2, $q = 6 \times 10^{-18}$ C, $E = 10^5$ V·m^{-1}, $K_1 = 0.5 + i$, $K_2 = 5 - 7i$, $\gamma_1 = 1 \times 10^{-7}$, $\gamma_2 = 300$, $\varepsilon = 0.8$, and $C = 0.05$.

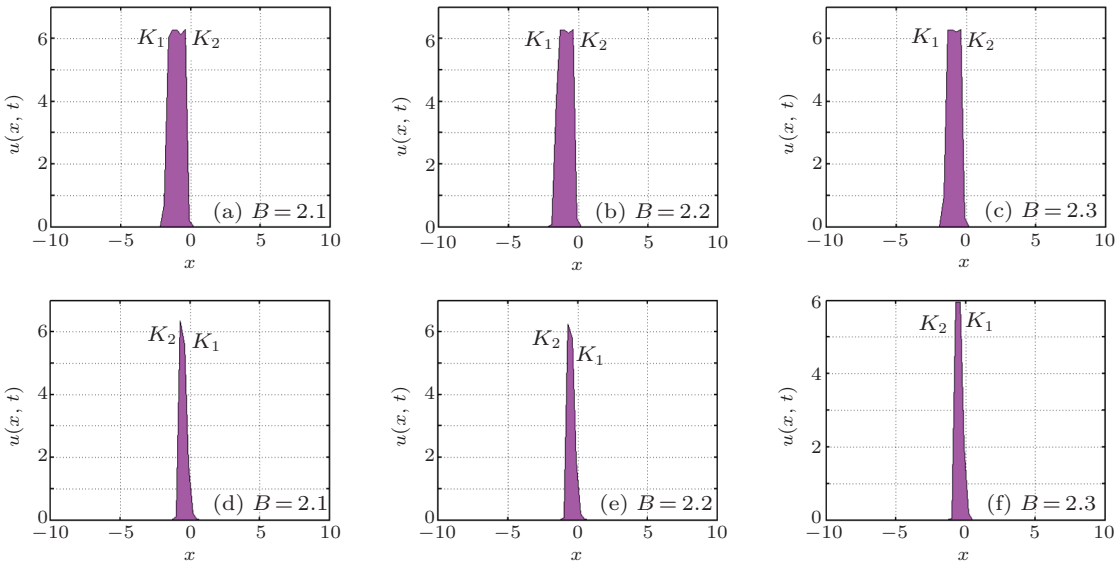


Fig. 6. (color online) Snapshots of inelastic collision between kink–antikink pair at two typical moments before collision at $t = -10$ ((a)–(c)) and after collision at $t = 10$ ((d)–(f)).

Figure 7 displays the snapshots of kink–antikink pair collision in microtubulin systems for the case of nonlinear quadratic inhomogeneity. Surprisingly in this case, the presence of nonlinear quadratic inhomogeneity makes the collision between the copropagating kink–antikink pair more inelastic resulting is an abrupt exchange of energy between the kinkons. Figure 8 depicts an exemplary collision scenario in the presence of quadratic inhomogeneity by varying the nonlinear coefficient A with the parameteric choices $\theta_1(0) = 0.001 - 10^{26}i$, $\theta_2(0) = 0.00009 + 10^{29}i$, $k = 0.0011$, $l = 8 \times 10^{-9}$ m, $R_0 = 10^{-8}$ m, $I = 1 \times 10^{-39}$ kg·m^2, $q = 6 \times 10^{-18}$ C, $E = 10^5$ V·m^{-1}, $K_1 = 1 \times 10^{-7} - 1.5 \times 10^{-6}i$, $K_2 = 5 \times 10^{-11} - 2i$, $\gamma_1 = 0.2 - 2i$, $\gamma_2 = 0.1 + i$, $\varepsilon = 0.009$, $C = 1$, and $B = 0.1$. From Fig. 8, it is evident that after collision, there is a suppression of energy profiles of the colliding kink–antikink pair, leading the collision perfectly inelastic.

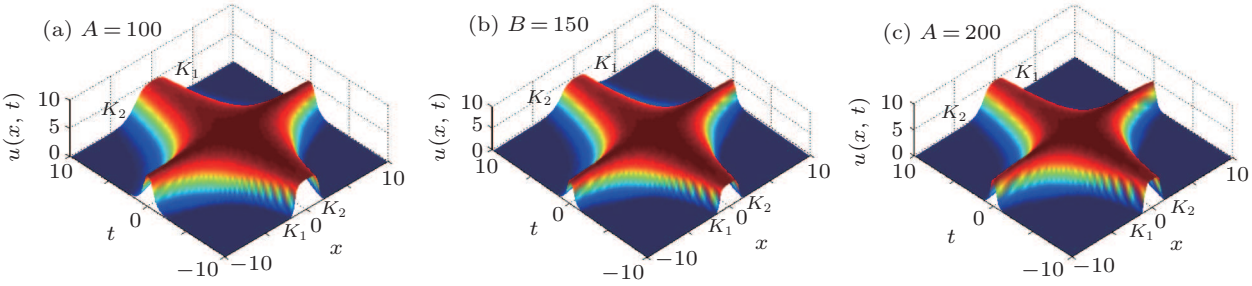


Fig. 7. (color online) Snapshots of inelastic collision between kink–antikink pair for various values of parameters $\theta_1(0) = 0.001 - 10^{26}i$, $\theta_2(0) = 0.00009 + 10^{29}i$, $k = 0.0011$, $l = 8 \times 10^{-9}$ m, $R_0 = 10^{-8}$ m, $I = 1 \times 10^{-39}$ kg·m^2, $q = 6 \times 10^{-18}$ C, $E = 10^5$ V·m^{-1}, $K_1 = 10^{-7} - 1.5 \times 10^{-6}i$, $K_2 = 5 \times 10^{-11} - 2i$, $\gamma_1 = 0.2 - 2i$, $\gamma_2 = 0.1 + 1i$, $\varepsilon = 0.009$, $C = 1$, and $B = 0.1$.

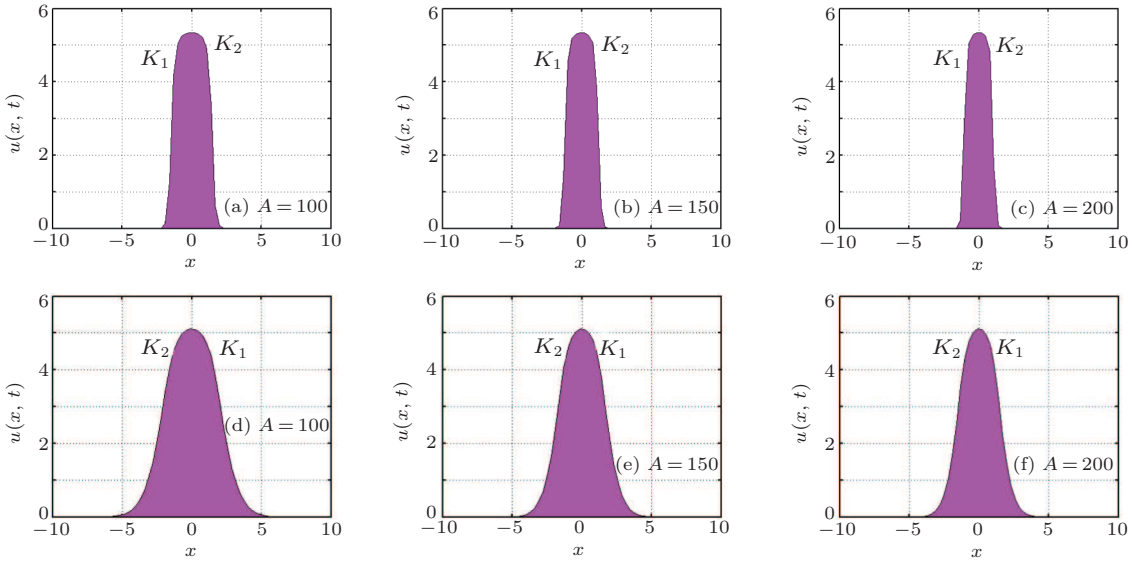


Fig. 8. (color online) Snapshots of inelastic collision between kink–antikink pair at two typical moments before collision at $t = -10$ ((a)–(c)) and after collision at $t = 10$ ((d)–(f)).

Simultaneously, we have plotted G and F for three soliton solutions under the influence of linear inhomogeneity in the form of $Bx + C$ which is shown in Figs. 9 and 10. Figure 9(a) indicates the snapshots of inelastic collision between the kink solitons at a particular region for various values of linear inhomogeneity parameter B and figure 10 displays the two-dimensional view of inelastic collision between kink solitons at two typical moments before collision at $t = -10$ and after collision $t = 10$. In Fig. 9, when the value of $B = 4.6$, the inelastic collision gives distinct pictures and as a result of an inelastic collision, there is an abrupt exchange of energy among the MT dimers and the kink solitons K_1, K_2 and K_3 emerge with an increase of energies as shown in Figs. 9(a) and 10(a). By increasing the value of $B = 5.1$, the kink solitons K_1 and K_3 energy seem to be increased and K_2 is decreasing which is depicted in Figs. 10(b) and 10(e). Very interestingly, the kink solitons K_1, K_2, and K_3 energies found to be increased by increasing the value of $B = 5.5$ which is portrayed in Figs. 10(c) and 10(f). We also try to understand the dynamics under influence of nonlinear inhomogeneity of the form $Ax^2 + Bx + C$ on the energy sharing mechanism between the kink solitons propagating along the MT protofilaments. Figures 11 and 12

portray an exemplary collision scenario for varying the values of nonlinear inhomogeneity parameter A. Figure 11(a) is plotted for $A = 15.1$, and from Fig. 12(a), it could be observed that three kink solitons K_1 emerge with the increase in energy, K_2 shows neither increase nor decrease in energy and K_3 emerges with the decrease in energy as depicted in Figs. 11(a), 12(a), and 12(d). Finally, we have compared the solutions obtained by both the methods (antikink soliton from double exp-function method and kink soliton from Hirota's bilinearization method) and presented them in Fig. 13.

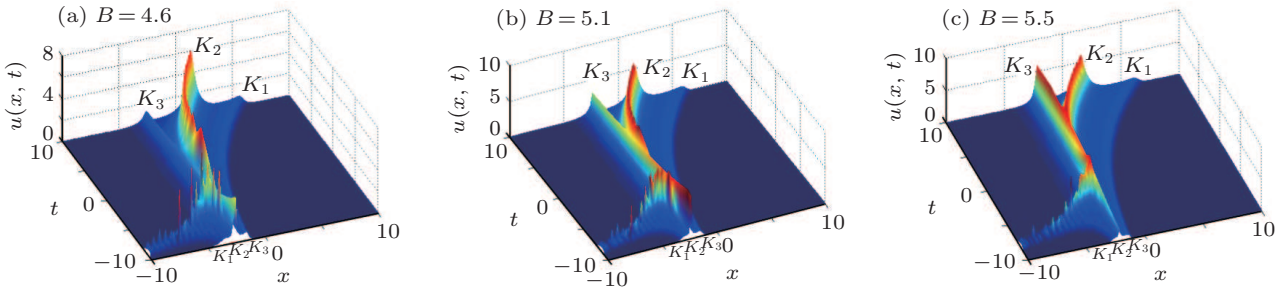


Fig. 9. (color online) Snapshots of inelastic collision between three kink solitons for various values of parameters $\theta_1(0) = 0.1 + i$, $\theta_2(0) = 0.3 + 10^{31}i$, $\theta_3(0) = 1.92 - i$, $k = 9 \times 10^{-5}$, $l = 8 \times 10^{-9}$ m, $R_0 = 10^{-8}$ m, $I = 1 \times 10^{-39}$ kg·m^2, $q = 6 \times 10^{-18}$ C, $E = 10^5$ V·m^{-1}, $K_1 = 4 + 9i$, $K_2 = 1 + 0.09i$, $K_3 = 0.009i$, $\gamma_1 = 0.9i$, $\gamma_2 = 1 - i$, $\gamma_3 = 0.001i$, $\varepsilon = 0.08$, and $C = 0.08$. (a) $B = 4.6$, (b) $B = 5.1$, (c) $B = 5.5$.

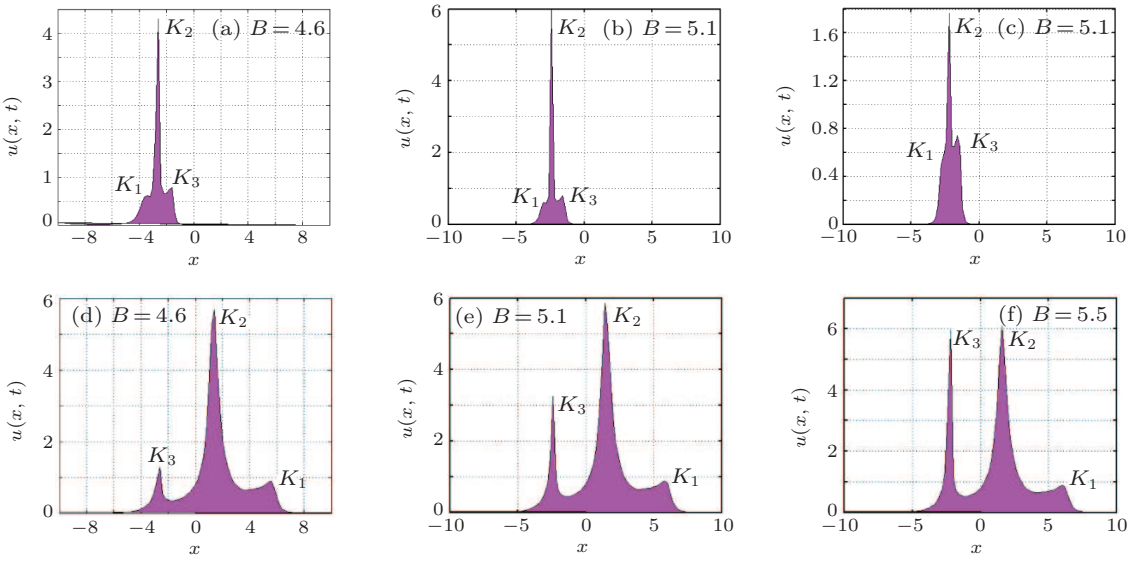


Fig. 10. (color online) Snapshots of inelastic collision between three kink solitons at two typical moments before collision at $t = -10$ ((a)–(c)) and after collision at $t = 10$ ((d)–(f)).

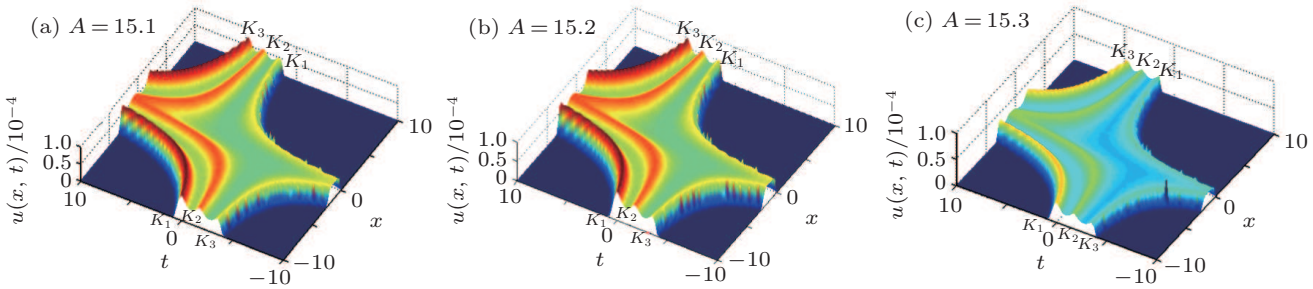


Fig. 11. (color online) Snapshots of inelastic collision between three kink solitons for various values of parameters $\theta_1(0) = 11.5 - i$, $\theta_2(0) = 6 + i$, $\theta_3(0) = 0.9 - i$, $k = 20$, $l = 8 \times 10^{-9}$ m, $R_0 = 10^{-8}$ m, $I = 1 \times 10^{-39}$ kg·m^2, $q = 6 \times 10^{-18}$ C, $E = 10^5$ V·m^{-1}, $K_1 = 0.03 + i$, $K_2 = 2i$, $K_3 = 2.9 - 5i$, $\gamma_1 = 0.000005i$, $\gamma_2 = 0.0001i$, $\gamma_3 = 1 + i$, $\varepsilon = 0.05$, $C = 0.1$, and $B = 26$. (a) $A = 15.1$, (b) $A = 15.2$, (c) $A = 15.3$.

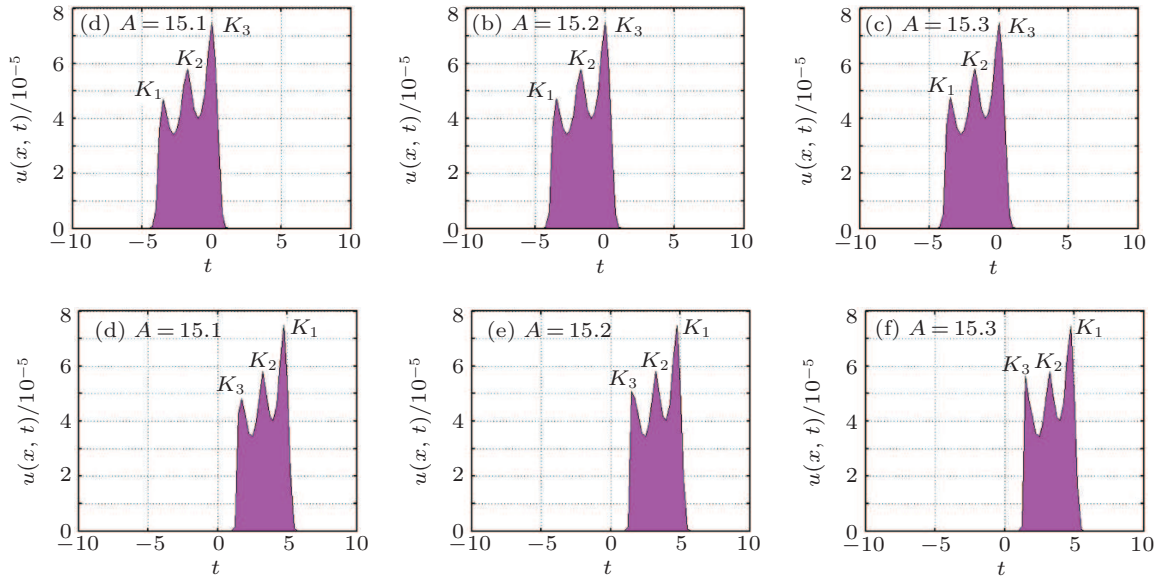


Fig. 12. (color online) Snapshots of inelastic collision between three kink solitons at two typical moments before collision at $x = -10$ ((a)–(c)) and after collision at $x = 10$ ((d)–(f)).

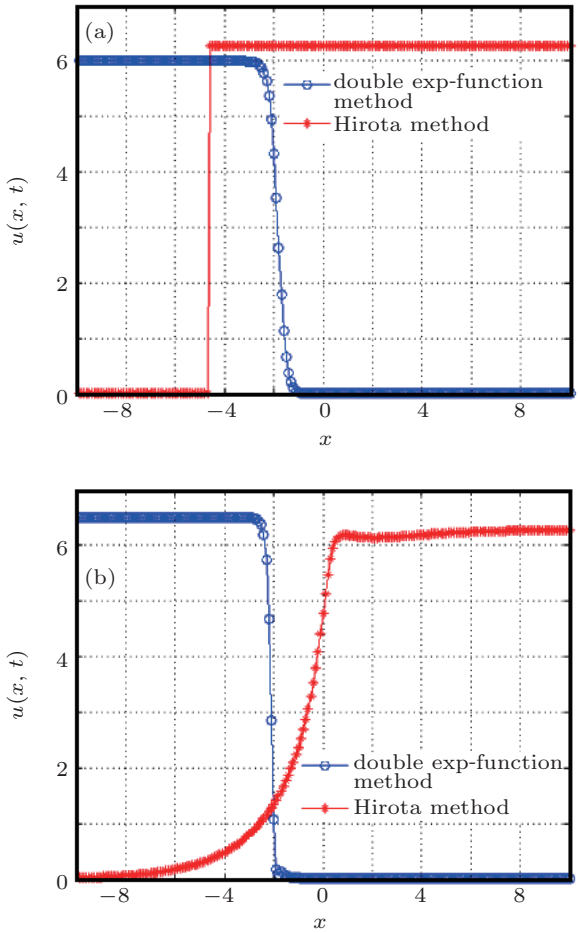


Fig. 13. (color online) The comparison of the solutions $u(x,t)$ of the two methods (double exp-function method and Hirota's bilearization method), (a) $t = -1$ for linear inhomogeneity and (b) $t = 1$ for nonlinear inhomogeneity.

Sataric *et al.*[13] already reported that the kink soliton formation is mainly due to the hydrolysis of GTP into GDP, so that hydrolysis corresponds to the conformational change resulting in the formation of a single kinkon. The propagation of a kink like excitation will then distribute the energy of hydrolysis at the preferred end of a MT. The creation and propagation of kink and antikink solitons in MTs may give a different picture of understanding the peculiar dynamical effect known as "treadmilling", originally proposed by Wegner. In contrast, Walker *et al.*[62] and Grego *et al.*[63] have suggested that biased polar dynamic instability of growing and shortening at both microtubule ends, with net growing occurring at one end and net shortening occurring at the opposite end creates the effect of treadmilling. The biased polar dynamic instability at opposite microtubule ends can give rise to net growth at one end of a microtubule and net shortening at the opposite end confirmed by fluorescence speckle microscopy.[63] In fact, when fluorescence speckle microtubules were attached to glass slides by kinesin motor proteins and the dynamic instability excursions at the opposite microtubule ends analyzed, many of the microtubules achieved treamilling both in a plus to minus direction and in a minus-to-plus direction. We expect that the process of polymerization and depolymerization of heterodimers in MTs may be highly assisted by the propagation of kink and antikink solitons respectively, as shown in Fig. 14. During cell division, chromosomes travel along MTs from the metaphase plate to the spindle poles, and MTs in one half spindle slide past anti-parallel MTs of the other half spindle. Following fertilization and conjugation in unicellular species, nuclei must travel toward one another as a prelude to fusion. To generate the forces for most, if not all, of these movements, the cell relies upon mechanochemical enzymes known as "microtubule motor proteins". In vitro motility assays have implicated two microtubule simulated ATPases, kinesin and dynein, as motors for microtubule-based transport. A kinesin is a protein belonging to a class of motor proteins found in eukaryotic cells. Ki-

nesins move along microtubule filaments, and are powered by the hydrolysis of ATP. The active movement of kinesins supports several cellular functions including mitosis, meiosis and transport of cellular cargo, such as in axonal transport. Most kinesins walk towards the plus end of a microtubule, which, in most cells, entails transporting cargo from the center of the cell towards the periphery. This form of transport is known as anterograde governed by the motion of antikink soliton as represented in the diagramatic representation Fig. 15 of movement of motor proteins.

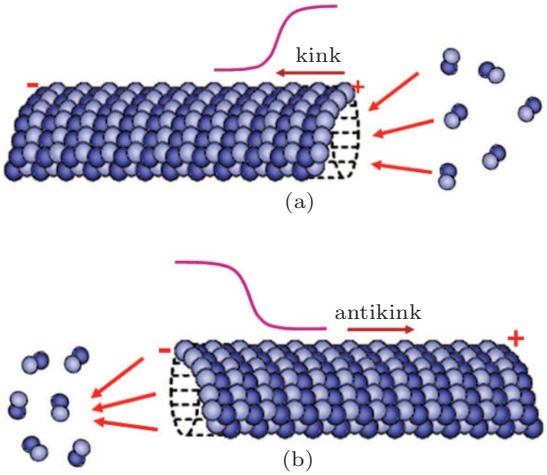


Fig. 14. (color online) (a) Polymerization of microtubules, (b) depolymerization of microtubules.

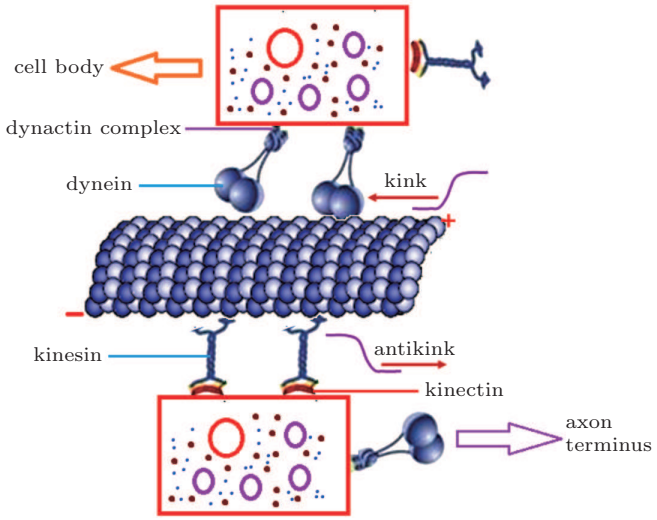


Fig. 15. (color online) Diagrammatic representation of kinesin and dynein movements along the microtubules.

The head is the signature of kinesin and its amino acid sequence is well conserved among various kinesins. Each head has two separate binding sites: one for the microtubule and the other for ATP. ATP binding and hydrolysis as well as ADP release change the conformation of the microtubule-binding domains and the orientation of the neck linker with respect to the head; this results in the motion of the kinesin which is shown in Fig. 15. Kinesins transport such cargo by walking unidirectionally along microtubule tracks hydrolysing one molecule of adenosine triphosphate (ATP) at each step.[64] It was thought that ATP hydrolysis powered each step, the energy released propelling the head forwards to the next binding site.[65] However, it has been proposed that the head diffuses forward and the force of binding to the microtubule is what pulls the cargo along.[66] There is a significant evidence that cargoes in-vivo are transported by multiple motors.[67,68] Kinesin accomplishes transport by "walking" along a microtubule. Two mechanisms have been proposed to account for this movement. In the "hand-over-hand" mechanism, the kinesin heads step past one another, alternating the lead position. In the "inchworm" mechanism, one kinesin head always leads, moving forward a step before the trailing head catches up. Despite some remaining controversy, mounting experimental evidence points towards the hand-over-hand mechanism as being more likely.[69] ATP binding and hydrolysis cause kinesin to travel via a "see-saw mechanism" about a pivot point.[70] This see-saw mechanism accounts for observations that the binding of the ATP to the no-nucleotide, microtubule-bound state results in a tilting of the kinesin motor domain relative to the microtubule. The living cells contain dynein regarded as motor protein are responsible for converting the chemical energy present in ATP into the mechanical energy for motion. Dynein is considered as "walking" protein as it transports various chemical cargo by walking along cytoskeletal microtubules proceeding towards the negative end of the microtubule (or minus end) which is usually oriented towards the cell center. This active processing are termed to be "minus-end directed motors", which is the counterpart for kinesins. Kinesins are another kind of motor proteins that move towards the microtubule's positive end (or plus end) are called plus-end directed motors as represented schematically in Fig. 15. Sliding of microtubules in the axonemes of cilia and flagella is due to the presence of axonemal dynein and is found only in cells that have those structures. As an active participants in organelle transport and centrosome assembly, cytoplasmic dynein are the cause for such transport and they have their high survival in all animal cells and possibly plant cells.[71] Cytoplasmic dynein are set in motion progressively along the microtubule; i.e., one or the other of its stalks is always attached to microtubule thereby leading the dynein to walk along the microtubule with detaching. In addition, these are highly probable in locating the position of Golgi complex and other organelles in the cell.[71] It also aid to transport the essential cargo needed for all cell function such as vesicles made by the endoplasmic reticulum, endosomes and lysosomes.[72]

As it is termed, motor protein, dynein also involved in the movement of chromosomes, locating the mitotic spindles for cell division, carrying organelles and microtubule fragments along the axons of neurons in axoplasmic transport process. The intermolecular assembly of dynein motor is composed of

many smaller polypeptides subunits and these components are also present in cytoplasmic and axonemal dynein with some unique subunits. The dynamical force required for ATPase activity of each dynein heavy chain is primarily located in its large doughnut-shaped "head", with its two projections from the head connect it to other cytoplasmic structures. One projections, the coiled-coil stalk bind to and walks along the microtubule surface through the repetitive process called detachment and reattachment. While the other projection, also called extended tail or stem, binds to the intermediate and light chain subunits which attach the dynein to its cargo. Another interesting activity of the heavy chain cytoplasmic dynein motor is that it motivate a single dynein molecule to transfer its cargo by means of walking for a considerable distance aside the microtubule without becoming completely detached. The dynactin, another multisubunit protein which is essential for mitosis activate the cytoplasmic dynein present in the eukaryotes. The presence of dynactin is responsible to regulate the activity of dynein and also actively facilitates the attachment of dynein to its cargo. The AAA ATPase motor domain undergoes a conformational change during the power stroke which causes movement and these conformational changes causes pivotal joint between microtubule-binding stalk and cargo-binding tail with sliding of microtubules relative to each other. This sliding causes bending a critical requirement for cilia to beat and propel the cell or other particles. Dynein molecules that move in opposite direction probably are activated and deactivated in a collective fashion so that propagation of kink soliton assists the cilia or flagella oscillatory motion highly as shown in Fig. 15. The radial spoke fills the synchronization of this movement.

5. Conclusions

In this paper, we studied the nonlinear dynamics of the inhomogeneous microtubulin systems in the presence of a variety of competing nonlinear inhomogeneities. In MTs, inhomogeneity may arise because of a local distortion that can be due to an attached associated protein or a structural discontinuity in the MT. Local inhomogeneities in MTs can be relevant to many biological processes such as energy transition of guanine triphosphate (GTP) hydrolysis, cell growth, excitation and inhibition of neurons, and respiratory infection. The dynamical equation, which finally appeared in the form of a perturbed sine-Gordon equation admitting kink-type and antikink type soliton solutions, was derived from a suitable Hamiltonian. We demonstrated the collision scenario between kink–antikink pair and bring out clearly the various features underlying the fascinating inelastic and elastic collision under the influence of linear and nonlinear inhomogeneity respectively. The MT is a highly dynamic polymer that continuously exchange heterodimers by the mechanism of dynamic instability and by treadmilling. After polymerization, GTP bound to the β-tubulin in the heterodimer is hydrolyzed to GDP and considerable amount of energy is stored in the MT. It is known that energy produced during GTP hydrolysis is delivered to MTs and may be used for the increase of tension in the MT, may excite kink–antikink solitons. These kink and antikink solitons are envisaged as a control mechanism for the movement of microtubule motor proteins such as kinesins and dyneins which generally move in opposite directions along a microtubule which involved in organelle transport, in mitosis, in meiosis and in the transport of synaptic vesicles along axons.

Acknowledgments

One of the author L. K gratefully acknowledges the financial support from UGC in the form of a research award, NBHM, India in the form of a major research project, BRNS, India in the form of a Young Scientist Research Award and ICTP, Italy in the form of a Junior Associateship. A. M gratefully acknowledges UGC for Rajiv Gandhi National Fellowship.

References

[1] Alberts B, Bray D, Lewis J, Raff M Roberts K and Watson J 2005 *Molecular Biology of the Cell* (New York & London: Garland publishing)
[2] Jorden M A and Wilson L 2004 *Nat. Rev. Cancer* **4** 253
[3] Mollinedo F and Gajate C 2003 *Apoptosis* **8** 413
[4] Gomez A M, Kerfant B G and Vasort G 2000 *Circ. Res.* **86** 30
[5] Rappaport L and Samuel J L 1998 *Int. Rev. Cytol.* **113** 101
[6] Webster D R and Patrick D L 2000 *Am. J. Physiol. Heart Circ.* **278** H1653
[7] Yonemochi H, Saikawa T, Takakura T, Ito S and Takaki R 1990 *Circulation* **81** 1401
[8] Webster D R 2002 *Cardiovasc Toxicol* **2** 75
[9] Tuszyński J A, Trpisová B, Sept D and Satarić M V 1997 *Biosystems* **42** 153
[10] Stebbings H and Hunt C 1982 *Cell Tiss. Res.* **227** 609
[11] Chretien D, Fuller S D and Karsenti E 1995 *J. Cell Biol.* **129** 1311
[12] Chou K C, Zhang C T and Maggiora G M 1994 *Biopolymers* **34** 143
[13] Satarić M V, Tuszyński J A and Žakula R B 1993 *Phys. Rev. E* **48** 589
[14] Vinckier A, Dumortier C, Engelborghs Y and Hellemans L 1996 *J. Vac. Sci. Technol. B Microelectron. Nanometer Struct. Process. Meas. Phenom.* **14** 1427
[15] Kurachi M, Hoshi M and Tashiro H 1995 *Cell Motil. Cytoskeleton* **30** 221
[16] Dye R B, Fink S P and Williams R C J 1993 *J. Biol. Chem.* **268** 6847
[17] Gittes F, Mickey B, Nettleton J and Howard J 1993 *J. Cell Biol.* **120** 923
[18] Elbaum M, Fygenson D K and Libchaber A 1996 *Phys. Rev. Lett.* **76** 4078
[19] Nogales E, Whittaker M, Milligan R A and Downing K H 1999 *Cell* **96** 79
[20] Howard J 2001 *Sinauer* (Associates, MA)
[21] Mandelkow E M, Mandelkow E and Milligan R A 1991 *J. Cell Biol.* **114** 977
[22] Satarić M V and Tuszyński J A 2005 *J. Biol. Phys.* **31** 487
[23] Pierobon P, Mobilia M, Kouyos R and Frey E 2006 *Phys. Rev. E* **74** 031906
[24] Kolomeisky A B 1998 *J. Phys. A: Math. Gen.* **31** 1153
[25] Chou T and Lakatos G 2004 *Phys. Rev. lett.* **93** 198101
[26] Trpisová B and Tuszynski J A 1997 *Phys. Rev. E* **55** 3288
[27] Huang S and Ingber D E 1999 *Nat. Cell Biol.* **1** E131
[28] Kullander K 2005 *Trends Neurosci.* **28** 239
[29] Estrella B, Estrella R, Oviedo J, Narvaez X, Reyes M T, Gutierrez M and Naumova E N 2005 *Ecuador. Environ. Health Perspect.* **113** 607

[30] Ablowitz M J, Kaup D J, Newell A C and Segur H 1974 *Stud. Appl. Math.* **53** 249
[31] Athenstaedt H 1974 *Ann. N. Y. Acad. Sci.* **238** 68
[32] Margulis L, To L and Chase D 1978 *Science* **200** 1118
[33] Mickey B and Howard J 1995 *J. Cell Biol.* **130** 909
[34] Frȟlich H 1996 *Modern Bioelectrochemistry* edited by Guttman F and Keyzer H (New York)
[35] Barnett M P 1987 *Molecular Systems to Process Analog and Digital Data Assosiatively* (Washington, DC: Naval Research Laboratory)
[36] Marx A and Mandelkow E 1994 *European Biophys. J.* **22** 405
[37] Miura M R 1978 *Bcklund Transformation* (Berlin: Springer-Verlag)
[38] Gu C H, Hu H S and Zhou Z X 1999 *Darboux Transformation in Solitons Theory and Geometry Applications* (Shanghai: Shanghai Science Technology Press)
[39] Gardner C S, Greene C S, Kruskal M D and Miura R M 1967 *Phys. Rev. Lett.* **19** 1095
[40] Hirota R 1971 *Phys. Rev. Lett.* **27** 1192
[41] Malfliet W 1992 *Am. J. Phys.* **60** 650
[42] Kavitha L, Srividya B and Gopi D 2010 *J. Magn. Magn. Mater.* **322** 1793
[43] Kavitha L, Akila N, Srividya B and Gopi D 2010 *Nonl. Sci. Lett. A* **1** 95
[44] Kavitha L, Jayanthi S, Muniyappan A and Gopi D 2011 *Phys. Scr.* **84** 035803
[45] Kavitha L, Venkatesh M, Jayanthi S and Gopi D 2012 *Phys. Scr.* **86** 025403
[46] Zdravković S, Kavitha L, Satarić M V, Zeković S and Petrović J 2012 *Chaos Soliton. Fract.* **45** 1378
[47] Gepreel K A and Omran S 2012 *Chin. Phys. B* **21** 110204
[48] Kavitha L, Akila N, Prabhu A, Kuzmanovska-Barandovska O and Gopi D 2011 *Math. Comput. Modelling* **53** 1095
[49] Wang M L 1996 *Phys. Lett. A* **213** 279
[50] Yan Z and Zhang H Q 2001 *Phys. Lett. A* **285** 355
[51] Yan Z Y 2003 *Chaos Soliton. Fract.* **18** 299
[52] Kavitha L, Saravanan M, Srividya B and Gopi D 2011 *Phys. Rev. E* **84** 066608
[53] Zeković S, Muniyappan A, Zdravković S and Kavitha L 2014 *Chin. Phys. B* **23** 020504
[54] He J H and Wu X H 2006 *Chaos Soliton. Fract.* **30** 700
[55] He J H and Abdou M A 2007 *Chaos Soliton. Fract.* **34** 1421
[56] Wu X H and He J H 2007 *Comput. Math. Appl.* **54** 966
[57] Fu H M and Dai Z D 2009 *Int. J. Nonlinear Sci. Numer. Simul.* **10** 927
[58] Ma W X, Huang T W and Zhang Y 2010 *Phys. Scr.* **82** 065003
[59] Kavitha L, Srividya B and Gopi D 2011 *Comput. Math. Appl.* **62** 4691
[60] Hirota R 1973 *J. Math. Phys.* **14** 805
[61] Zhou Z J, Fu J Z and Li Z B 2010 *Appl. Math. Comput.* **217** 92
[62] Walker R A, O'Brien E T, Pryer N K, Soboeiro M F, Voter W A and Erickson H P 1988 *J. Cell Biol.* **107** 1437
[63] Grego S, Cantillana V and Salmon E D 2001 *Biophys. J.* **81** 66
[64] Schnitzer M J and Block S M 1997 *Nature* **388** 386
[65] Vale R D and Milligan R A 2000 *Science* **288** 88
[66] Mather W H and Fox R F 2006 *Biophys. J.* **91** 2416
[67] Gross S P, Vershinin M and Shubeita G T 2007 *Curr. Biol.* **17** R478
[68] Hancock W O 2008 *Curr. Biol.* **18** R715
[69] Asbury C L 2005 *Curr. Opinion in Cell Biol.* **17** 89
[70] Sindelar C V and Downing K H 2010 *Proc. Natl. Acad. Sci. USA* **107** 4111
[71] Karp G, Vogel S, Kuhlmann-Krieg S and Beginnen K 2005 *Molekulare Zellbiologie* (Springer-Lehrbuch)
[72] Karp G 2005 *Cell and Molecular Biology: Concepts and Experiments* (4th edn.) (Hoboken, New Jersey: John Wiley and Sons) p. 598)